Molecular Cell, Volume *31*

Supplemental Data

Diversity-Generating Retroelement Homing Regenerates Target Sequences for Repeated Rounds of Codon Rewriting and Protein Diversification

Huatao Guo, Longping V. Tse, Roman Barbalat, Sameer Sivaamnuaiphorn, Min Xu, Sergei Doulatov, and Jeff F. Miller

Supplemental Experimental Procedures

Oligonucleotides

List of oligonucleotides used in this study:

Name	Sequence
P1	5' CCCTCTAGAGCTCCGGTTGCTTGTGGACG
P2	5' AGCAAGCTTCCTCGATGGGTTCCAT
P3	5' ATATCTAGACGTTTTCTTGGGTCTACCGTTTAATGTCG
P4	5' ATAAAGCTTCGACATTAAACGGTAGACCCAAGAAAA
P5	5' AAATCTAGATCTGTCTGCGTTTGTGTT
P6	5' AGCAAGCTTAGCACAGGAACACAAACG
P7	5' CCCTCTAGAATTCCAGGCGCTGGCTTTC
P8	5' AGCGGATCCGAAGCAGGACAGAACCG
P9	5' AGCGGATCCACCTATTGAGGAAAGGC
P10	5' AAATCTAGACGCTGCTGCGCTATTCGGCGGC
E1s	5' ATATCTAGACGGGCCGTCGAAGTCGACGTTTTCTTG
E2a	5' ATAAAGCTTCGCGTTCGAGGTCGACATTAAACGG
*td*E2	5' AGGTCGACATTAAACGGT

Bacterial strains and phages

B. bronchiseptica RB50, RB53Cm, and RB54 have been previously described (Liu et al., 2004). Strain RB50Δ*recA* was constructed by deleting the entire *recA* ORF via allelic exchange. The BPP-1d lysogen was constructed from an RB50 BPP-1 lysogen (ML6401) (Liu et al., 2004) by deleting sequences from the 5' end of TR to position 882 of *brt*. BPP-1dΔVR1-99 and BPP-1dΔVR1-99IMH* lysogens were constructed from BPP-1d, and both have a deletion of VR from position 1 to 99. In the latter construct, the IMH in VR was replaced by IMH* from TR. Phage BPP-1 has been described previously (Liu et al., 2004) and derivative phages are produced from the above lysogens.

Plasmid constructs

Plasmid donors used in DGR homing assays were derived from pMX1, which expresses the BPP-1 *atd*, *TR*, and *brt* loci under control of an *fhaB* promoter (Xu et al., in preparation). pMX1 includes a pBBR1 replication origin and confers chloramphenicol resistance (Antoine and Locht, 1992). pMX1/SMAA is an RT-deficient mutant of pMX1

with the YMDD box in the *brt* ORF replaced with amino acid residues SMAA (Liu et al., 2002).

pMX1b is a derivative of pMX1 with the SalI restriction site in the polylinker between the *fhaB* promoter and *atd* eliminated via SalI restriction, filling-in by T4 DNA polymerase and religation. Plasmids pMX-TG1a, pMX-TG1b and pMX-TG1c are derivatives of pMX1b with a 36 bp sequence (5'-GTCGACGTTTTCTTGGGTCTACCGTTTAATGTCGAC) inserted at TR positions 19, 47 and 84, respectively. The 36 bp sequence includes 24 bp ligated exons of the phage T4 *td* group I intron flanked by SalI sites.

Plasmid pMX-*td* is derived from pMX-TG1c with the *td*Δ1-3 intron (a splicing-competent derivative of phage T4 *td* group I intron lacking most of the intron ORF) inserted between the exons (Cousineau et al., 1998). The intron was inserted in the same orientation as that of TR. Plasmids pMX-*td*/P6M3 and pMX-*td*/ΔP7.1-2a are derivatives of pMX-*td* with splicing-defective *td* introns. pMX-*td*/P6M3 has G78C and C79G substitutions, while pMX-*td*/ΔP7.1-2a carries a Δ877-908 deletion (Mohr et al., 1992). Plasmid pMX-*td*- has the *td* intron and its flanking exons inserted in the reverse orientation.

pMX-AvAp was constructed to facilitate introduction of mutations into TR and its flanking regions and was derived from pMX1b through site-directed mutagenesis. Sequences from *atd* position 336 to *brt* position 186 were replaced with the sequence 5'-CCTAGGCCGCGGGCCC to introduce AvrII and ApaI sites. To eliminate the AvrII and ApaI sites in the polylinker in front of the *atd* gene, sequence 5'-CCTAGGTACCGGGCCC was replaced with 5'-CCTAGATATCGGTCTC. Plasmid pMX-TG1c/AA was derived from pMX-AvAp and is essentially the same as pMX-TG1c, with the exception of AvrII and ApaI sites in *atd* and *brt* which were introduced by silent mutations. Silent mutations were verified not to affect DGR homing (pMX-TG1c/AA in Figure S6).

Plasmids used for TR internal deletion analysis in Figure 2 were constructed from the pMX-AvAp vector: pMX-ΔTR1-84, pMX-ΔTR11-84, pMX-ΔTR23-84 and pMX-ΔTR33-84 include 50 bp of the 3'-end TR (3' boundary at TR position 85), while having 0, 10, 22 and 32 bp of the 5'-end TR, respectively; pMX-ΔTR33-97 and pMX-ΔTR33-113 have 32 bp of the 5'-end TR, while having 38 and 21 bp of the 3'-end TR, respectively. Between the deletion junctions, all the constructs have a 32 bp sequence (5'-AGATCTGTCTGCGTTTGTGTTCCTGTGCTAGC) inserted as a tag (TG2) to facilitate DGR homing analysis. pMX-FL was constructed as a positive control, with TG2 inserted between positions 84 and 85 of the full-length TR.

Additional TR internal deletion constructs pMX-ΔTR20-47, pMX-ΔTR20-84 and pMX-ΔTR48-84 were derived from pMX-TG1a, pMX-TG1b and pMX-TG1c, and contain deletions between the insertions of TG1a and TG1b, TG1a and TG1c, and TG1b and TG1c, respectively. At the deletion junctions, the 36 bp TG1 tag was inserted to facilitate DGR homing assays.

Plasmids for silent mutation scanning to determine regions of the RNA transcript important for DGR homing were constructed from pMX-AvAp and are identical to pMX-TG1c/AA except for the silent mutations. Plasmids pMX-A1, pMX-A2 and pMX-A3 contain silent mutations in the *atd* ORF and have the 3'-end *atd* sequences 5'-ATTGCCCGC, 5'-GTGAATCGC and 5'-GCTGGGAAA replaced by 5'-ATTGCGAGG, 5'-GTGAACAGG and 5'-GCAGGCAAG, respectively. The *brt* ORF can potentially be extended at the 5' end to sequences upstream of *atd*. Plasmids pMX-T1, pMX-T2 and pMX-T3 contain silent mutations upstream of the *brt* ORF, and have the TR sequences 5'-CTGCTGCGC, 5'-TCGGGGCGC and 5'-CCCATCACC replaced by 5'-CTGCTCAGG,

5'-TCGGGAAGG and 5'-CCAATAACA, respectively. Plasmids pMX-T4, pMX-T5 and pMX-T6 contain silent mutations in sequences upstream of the *brt* ORF, and have the sequences 5'-CTTTCCTCA, 5'-ACGTCGATT and 5'-ACTTCTTCA in the spacer between TR and *brt* replaced by 5'-CTTAGTAGC, 5'-ACCAGCATA and 5'-ACTAGCAGC. Plasmids pMX-T7, pMX-T8 and pMX-T9 contain silent mutations in the *brt* ORF, and have the *brt* sequences 5'-AATCTGCTC, 5'-AAGCGCCGG and 5'-CTGCTGGCC replaced by 5'-AACCTCCTG, 5'-AAGAGAAGA and 5'-CTCCTCGCG.

Plasmids for marker transfer/coconversion studies were also constructed from pMX-AvAp and include pMX-TRC1T, pMX-TRC6T, pMX-TRC11T, pMX-TRC16T, pMX-TRC22T, pMX-TRC43T, pMX-TRC81T, pMX-TRC85T, pMX-TRC91T, pMX-TRC97T, pMX-TRC100T, pMX-TRC105T, pMX-TRC107T, pMX-TRC109T, pMX-TRC112T, pMX-TRC115T, pMX-TRC120T and pMX-TRC125T. They are identical to pMX-TG1c/AA except for the C to T substitutions at the indicated TR positions.

Plasmid pMX-M50 was derived from pMX-ΔTR23-84 and contains a 50 bp *mtd* sequence upstream of VR (*mtd* positions 952 to 1001) inserted at the BglII site downstream of TR position 22. Plasmid pMX-M50/SMAA is a Brt-deficient derivative of pMX-M50, with the essential YMDD box in the *brt* ORF replaced by SMAA.

Phage DNA Purification

To remove bacterial chromosomal and plasmid DNAs, phage lysates were treated with 50 μg/ml DNase I (Sigma) and 2.5 ng/ml micrococcal nuclease (Roche) in 10 mM Tris-HCl (pH 7.5), 1.0 mM $CaCl_2$, and 10 mM $MgCl_2$ at 37°C overnight. Aliquots were titrated to determine phage concentrations. Reactions were terminated by the addition of 5.0 mM EGTA and 5 ng/ml protease K followed by incubation at 37°C for ≥15minutes. Protease K was heat-inactivated at 70°C for ≥15 minutes. Samples were extracted with phenol-chloroform-isoamyl alcohol (Φ-CIA , 25:24:1) followed by chloroform extraction. For Mtd-defective phages, phage DNA concentrations were determined through quantitative PCR assays.

RNA Isolation for *td* intron splicing assays

Total RNAs were isolated from RB50 cells transformed with appropriate plasmids following induction in Stainer Scholte (SS) media containing 25 μg/ml of chloramphenicol (Cam), 20 μg/ml streptomycin (Str) (SS+Cam+Str) for 6 hours to express donor constructs. RNAs were isolated with trizol/$CHCl_3$ extraction and Φ-CIA (phenol-chloroform-isoamyl alcohol; 25:24:1) extraction, followed by ethanol precipitation. Subsequently, RNA samples were treated with Turbo DNase I (0.033 u/μl; Ambion) in 1X Turbo DNase I buffer at 37°C for 40 minutes to eliminate DNA contamination. Samples were then treated with protease K (17 μg/ml final concentration) at 37°C for 5 minutes to eliminate Turbo DNase I. RNAs were prepared by Φ-CIA extraction and ethanol precipitation.

Analysis of *td* intron RNA splicing in *B. bronchiseptica* by RT-PCR and primer-extension-termination assays

To analyze *td* intron RNA splicing by RT-PCR, cDNA products were first generated with primer P8 in a 20 μl reaction containing 50 mM Tris-HCl (pH 8.3), 75 mM KCl, 3 mM MgCl2, 5 mM DTT, 5% DMSO, 5 μg total RNAs, 10 u/μl Superscript III RT (Invitrogen) and 1.85 u/μl RNase Inhibitor (Amersham) at 50°C for 1 hour. Superscript III RT was then heat-inactivated at 70°C for 15 minutes. Subsequently, 2 μl cDNA products were amplified by PCR in a 50 μl reaction containing 60 mM Tris-SO_4 (pH 9.1), 18 mM $(NH_4)_2SO_4$ and 2 mM $MgSO_4$, 200 μM dNTPs, 5% DMSO, 6 ng/μl primers P9 and P10

each, and 0.5 μl Elongase Enzyme Mix (Invitrogen). PCR reactions were performed under the following condition: 1x (94^{o}C, 2 minutes); 15x (94^{o}C, 30 seconds; 50^{o}C, 30 seconds; 72^{o}C, 1 minute); 1x (72^{o}C, 10 minutes); 1x (4^{o}C, hold).

Relative amounts of precursor and spliced RNAs were measured through primer-extension-termination assay (Zhang et al., 1995) using Superscript III RT (invitrogen) and a *td* exon 2 primer (*td*E2).

Phage tropism switching assay

Progeny phages for tropism switching assays were generated from phage BPP-1d through single-cycle lytic infection of *B. bronchiseptica* RB50 or RB50Δ*recA* cells transformed with appropriate donor plasmids. To determine phage tropism switching frequencies, progeny phages were serially diluted and plaque-forming units on RB54 (Bvg^{-}) and RB53Cm (Bvg^{+}) cells were determined. Phage tropism switching frequencies were defined as the ratio of plaque-forming units on RB54 cells (Bvg^{-} tropism) vs. those on RB53Cm cells (Bvg^{+} tropism).

Total Nucleic Acid Purification

BPP-1dΔVR1-99 and BPP-1dΔVR1-99IMH* lysogens transformed with donor plasmids were grown overnight, modulated to the Bvg^{+} phase, and induced with 2 μg/ml mitomycin for 2 hours. Cells were precipitated, resuspended in 10 mM Tris-HCl (pH 8.0), 100 mM NaCl, 1 mM EDTA and 0.1% SDS. Total nucleic acids were purified by Φ-CIA extraction followed by chloroform extraction and ethanol precipitation. Pellets were resuspended in 10 mM Tris-HCl (pH 7.5), 1 mM EDTA and 10 ng/μl protease K. Following incubation at 37^{o}C for 30 minutes, samples were extracted with Φ-CIA and precipitated with ethanol.

Supplemental References

Antoine, R., and Locht, C. (1992). Isolation and molecular characterization of a novel broad-host-range plasmid from *Bordetella bronchiseptica* with sequence similarities to plasmids from gram-positive organisms. Mol Microbiol *6*, 1785-1799.

Cousineau, B., Smith, D., Lawrence-Cavanagh, S., Mueller, J.E., Yang, J., Mills, D., Manias, D., Dunny, G., Lambowitz, A.M., and Belfort, M. (1998). Retrohoming of a bacterial group II intron: mobility via complete reverse splicing, independent of homologous DNA recombination. Cell *94*, 451-462.

Liu, M., Deora, R., Doulatov, S.R., Gingery, M., Eiserling, F.A., Preston, A., Maskell, D.J., Simons, R.W., Cotter, P.A., Parkhill, J*., et al.* (2002). Reverse transcriptase-mediated tropism switching in *Bordetella* bacteriophage. Science *295*, 2091-2094.

Liu, M., Gingery, M., Doulatov, S.R., Liu, Y., Hodes, A., Baker, S., Davis, P., Simmonds, M., Churcher, C., Mungall, K*., et al.* (2004). Genomic and genetic analysis of *Bordetella* bacteriophages encoding reverse transcriptase-mediated tropism-switching cassettes. J. Bacteriol. *186*, 1503-1517.

Mohr, G., Zhang, A., Gianelos, J.A., Belfort, M., and Lambowitz, A.M. (1992). The *Neurospora* CYT-18 protein suppresses defects in the phage T4 td intron by stabilizing the catalytically active structure of the intron core. Cell *69*, 483-494.

Zhang, A., Derbyshire, V., Salvo, J.L., and Belfort, M. (1995). *Escherichia coli* protein StpA stimulates self-splicing by promoting RNA assembly in vitro. RNA *1*, 783-793.

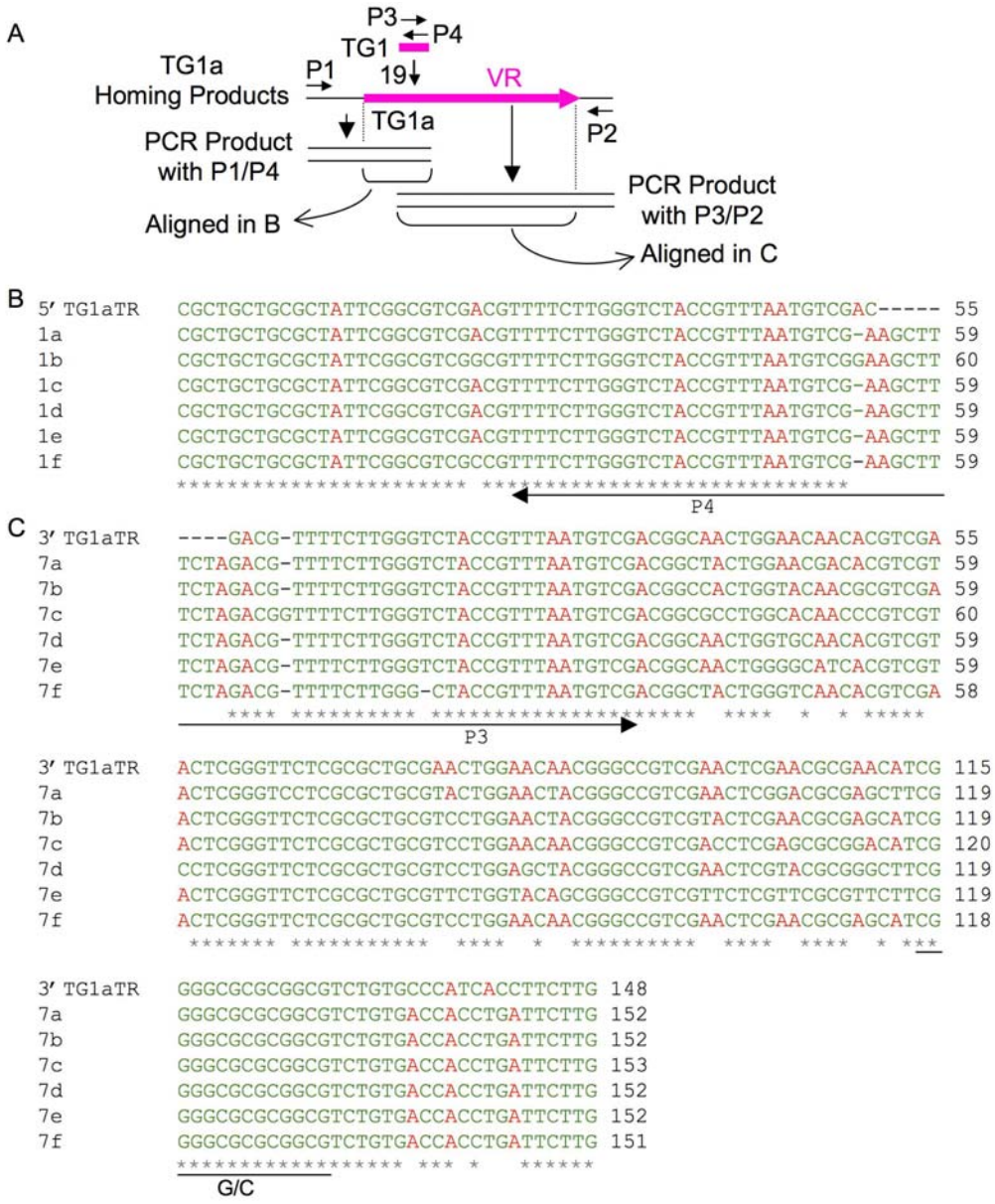

Figure S1. Alignment of plasmid pMX-TG1a homing products with TG1a TR sequences demonstrates adenine mutagenesis

(A) PCR detection strategy for pMX-TG1a homing products and regions of the products aligned in B and C. Primer annealing sites are indicated as small horizontal arrows.

(B) Alignment of the transferred TG1 tag and its upstream VR sequence to the corresponding TR region shows adenine mutagenesis.

(C) Alignment of the transferred TG1 tag and its downstream VR sequence to the corresponding TR region shows adenine mutagenesis.

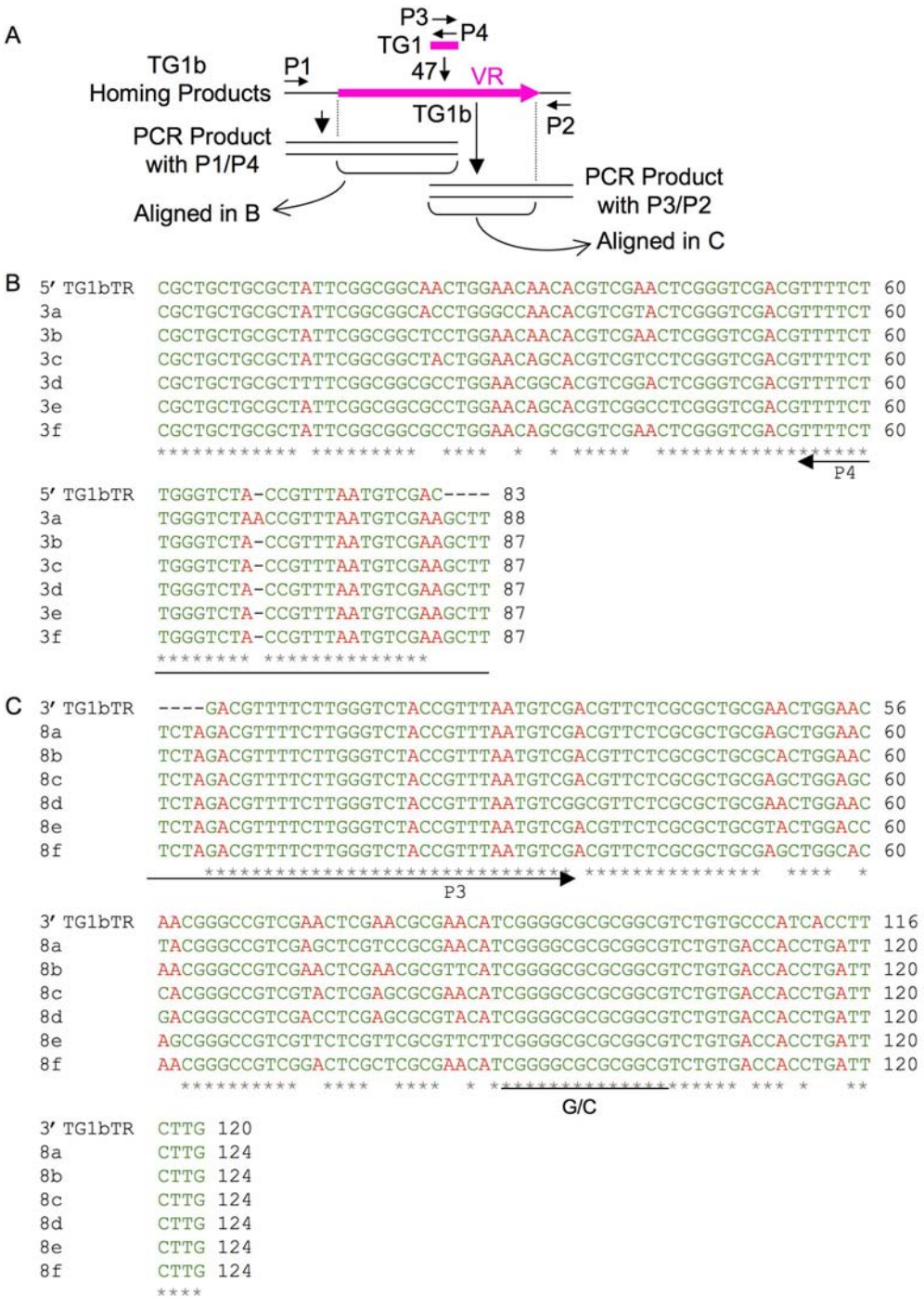

Figure S2. Alignment of plasmid pMX-TG1b homing products with TG1b TR sequences demonstrates adenine mutagenesis

(A) PCR detection strategy for pMX-TG1b homing products and areas of the products aligned in B and C. Primer annealing sites are indicated as small horizontal arrows.
(B) Alignment of the transferred TG1 tag and its upstream VR sequence to the corresponding TR region shows adenine mutagenesis.
(C) Alignment of the transferred TG1 tag and its downstream VR sequence to the corresponding TR region shows adenine mutagenesis.

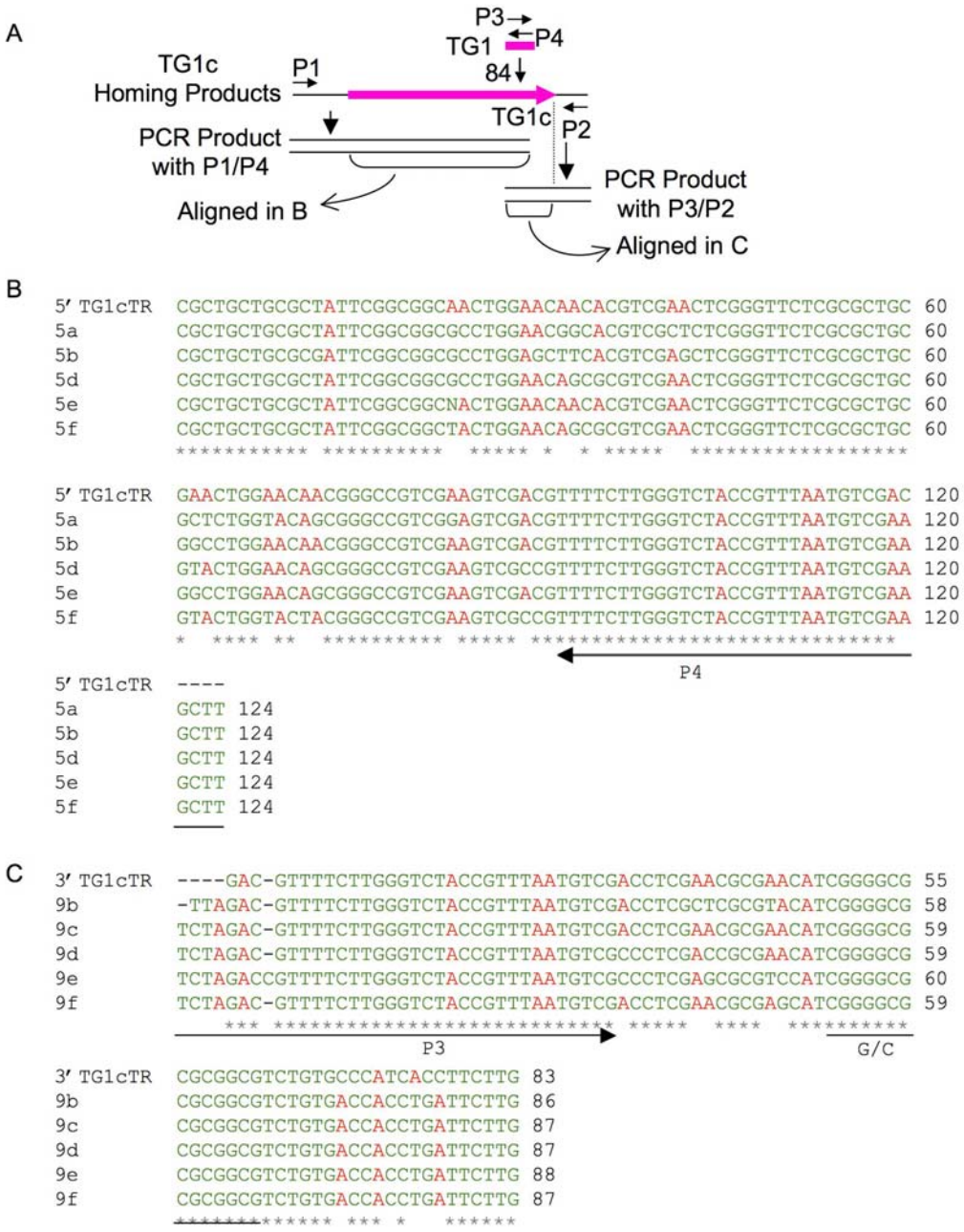

Figure S3. Alignment of plasmid pMX-TG1c homing products with TG1c TR sequences demonstrates adenine mutagenesis

(A) PCR detection strategy for pMX-TG1c homing products and areas of the products aligned in B and C. Primer annealing sites are indicated as small horizontal arrows.
(B) Alignment of the transferred TG1 tag and its upstream VR sequence to the corresponding TR region shows adenine mutagenesis.
(C) Alignment of the transferred TG1 tag and its downstream VR sequence to the corresponding TR region shows adenine mutagenesis.

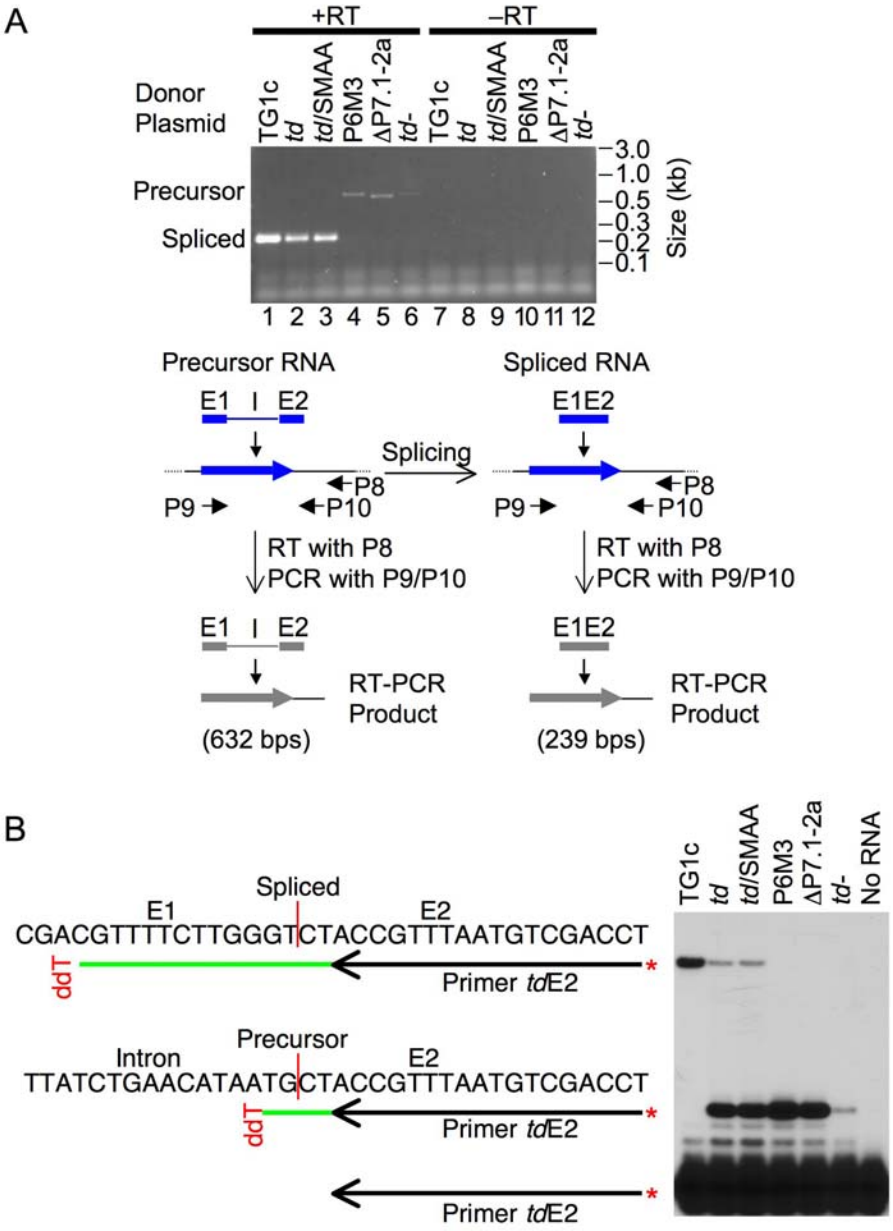

Figure S4. Phage T4 *td* intron self-splices in *B. bronchiseptica*
(A) Analysis of *td* intron RNA splicing by RT-PCR. Assays were performed with total RNAs isolated from *B. bronchiseptica* RB50 cells transformed with the indicated plasmids. Reverse transcription reactions with RNA samples were carried out with primer P8, and cDNA products were then amplified with primers P9 and P10 as diagramed below the gel. RT-PCR products of precursor and spliced RNAs are indicated to the left, and are 632 and 239 bp, respectively. Detection of these products required the presence of superscript III RT in the reverse transcription reaction. Sequence analysis of the spliced product from pMX-*td* (lane 2) did not show any sign of adenine mutagenesis (data not shown), suggesting that adenine-directed sequence diversification does not occur at the RNA level. TG1c, positive control pMX-TG1c; *td*,

pMX-*td*; *td*/SMAA, Brt-deficient mutant of pMX-*td;* P6M3 and ΔP7.1-2a, splicing-defective mutants; *td*-, donor with the *td* intron inverted.
(B) Quantitative analysis of *td* intron splicing through primer-extension-termination assays. 5'-^{32}P-labeled primer *td*E2 was used for primer extension assays in the presence of dATP, dCTP, dGTP and ddTTP (dideoxythymidine triphosphate), which terminates cDNA extension once incorporated. As the first adenine residues are located at different distances from the primer annealing sites in precursor and spliced RNAs, products of different sizes are produced and resolved by denaturing polyacrylamide gel, allowing accurate measurement of relative amounts of precursor and spliced RNAs. The primer and its extension products are indicated to the left. Donor plasmids are described in (A). The spliced products of pMX-*td* and the Brt-deficient pMX-*td*/SMAA are ~18% of the transcript levels of the positive control pMX-TG1c, which contains ligated *td* exons in TR.

A

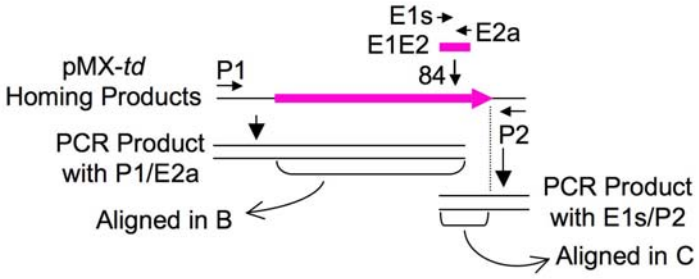

B

```
5′ TG1cTR  CGCTGCTGCGCTATTCGGCGGCAACTGGAACAACACGTCGAACTCGGGTTCTCGCGCTGC 60
3b         CGCTGCTGCGCTATTCGGCGGCGGCTGGAACAGCACGTCGAACTCGGGTTCTCGCGCTGC 60
3c         CGCTGCTGCGCTATTCGGCGGCGCCTGGAACTCCCCGTCGGACTCGGGTTCTCGCGCTGC 60
3d         CGCTGCTGCGCTATTCGGCGGCGCCTGGCGCAACACGTCGTCCTCGGGTTCTCGCGCTGC 60
3e         CGCTGCTGCGCGTTTCGGCGGCGCCTGGAACCACACGTCGAACTCGGGTTCTCGCGCTGC 60
3f         CGCTGCTGCGCTCTTCGGCGGCTACTGGAACAACCCGTCGAACTCGGGTTCTCGCGCTGC 60
3g         CGCTGCTGCGCTCTTCGGCGGCTACTGGAACAGCGCGTCGAACTCGGGTTCTCGCGCTGC 60
3h         CGCTGCTGCGCTTTTCGGCGGCTACTGGCTCCTCGCGTCGGCCTCGGGTTCTCGCGCTGC 60
3i         CGCTGCTGCGCTATTCGGCGGCGCCTGGAACAGCACGTCGAACTCGGGTGCTCGCGCTGC 60
3j         CGCTGCTGCGCTATTCGGCGGCAACTGGACCAACACGTCGTACTCGGGTTCTCGCGCTGC 60
3k         CGCTGCTGCGCTATTCGGCGGCGCCTGGAACTACACGTCGAACTCGGGTTCTCGCGCTGC 60
           ***********  *********  ****  *  * *****  ******* **********

5′ TG1cTR  GAACTGGAACAACGGGCCGTCGAAGTCGACGTTTTCTTGGGTCTACCGTTTAATGTCGAC 120
3b         GTCCTGGAGCTACGGGCCGTCGAAGTCGACGTTTTCTTGGGTCGCCCGTTTAATGTCGAC 120
3c         GTACTGGTCCAACGGGCCGTCGGAGTCGACGTTTTCTTGGGTCTGCCGTTTAATGTCGAC 120
3d         GTACTGGCTCGACGGGCCGTCGAAGTCGACGTTTTCTTGGGTCTCCCGTTTAATGTCGAC 120
3e         GAGCTGGAACTCCGGGCCGTCGAAGTCGACGTTTTCTTGGGTCGCCCGTTTAATGTCGAC 120
3f         GCTCTGGAACAGCGGGCCGTCGAAGTCGACGTGTTCTTGGGTCTGCCGTTTAATGTCGAC 120
3g         GGACTGGAACTACGGGCCGTCGCTGTCGACGTTTTCTTGGGTCTACCGTTTAATGTCGAC 120
3h         GGGCTGGAGCTCCGGGCCGTCGGGGTCGCCGTTTTCTTGGGTCGCCCGTTTAATGTCGAC 120
3i         GGCCTGGAACAGCGGGCCGTCGAAGTCGCCGTTTCCTTGGGTCGCCCGTTTAATGTCGAC 120
3j         GTCCTGGAACTACGGGCCGTCGAAGTCGACGTTTTCTTGGGTCTGCCGTTTAATGTCGAC 120
3k         GTACTGGAACTTCGGGCCGTCGAAGTCGACGTTTTCTTGGGTCTACCGTTTAATGTCGAC 120
           *  ****  *  **********  **** *** * ********  ***************
                                                      EJ        E2a

5′ TG1cTR  CTCGAACGC-GAACATC 136
3b         CTCGA-CGC-GAAGCTT 135
3c         CTCGAACGC-GAAGCTT 136
3d         CTCGAACGC-GAAGCTT 136
3e         CTCGAACGC-GAAGCTT 136
3f         CTCGAACGC-GAAGCTT 136
3g         CTCGAACGC-GAAGCTT 136
3h         CTCGAACGCCGAAGCTT 137
3i         CTCGAACGC-GAAGCTT 136
3j         CTCGAACG--GAAGCTT 135
3k         CTCGAACGC-GAAGCTT 136
           ***** **  ***  *
```

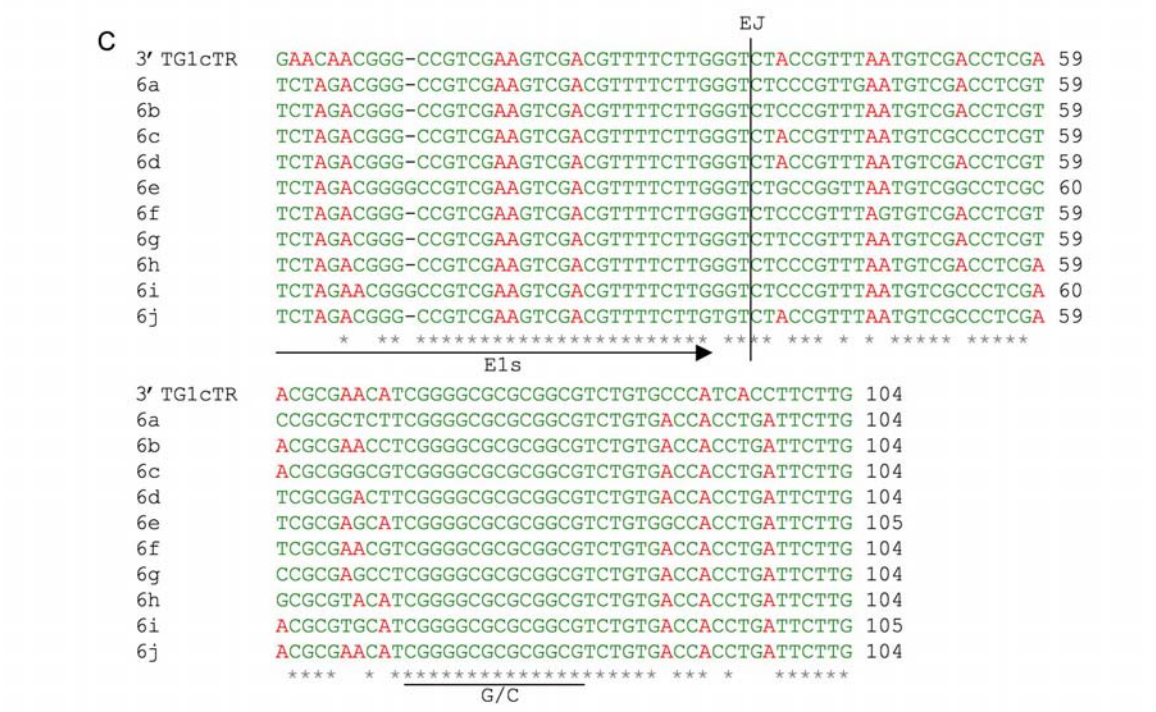

Figure S5. Alignment of plasmid pMX-*td* homing products with TG1c TR sequences shows precise exon ligation and adenine mutagenesis
(A) PCR detection strategy for pMX-*td* homing products and areas of the products aligned in B and C. Primer annealing sites are indicated as small horizontal arrows.
(B) Alignment of the transferred *td* exons and their upstream VR sequence to the corresponding TG1c TR region shows accurate exon joining and adenine mutagenesis. Primer E2a annealing site and exon junction (EJ) are also indicated.
(C) Alignment of the transferred *td* exons and their downstream VR sequence to the corresponding TG1c TR region shows accurate exon joining and adenine mutagenesis. Primer E1s annealing site, EJ and the $(G/C)_{14}$ element are indicated.

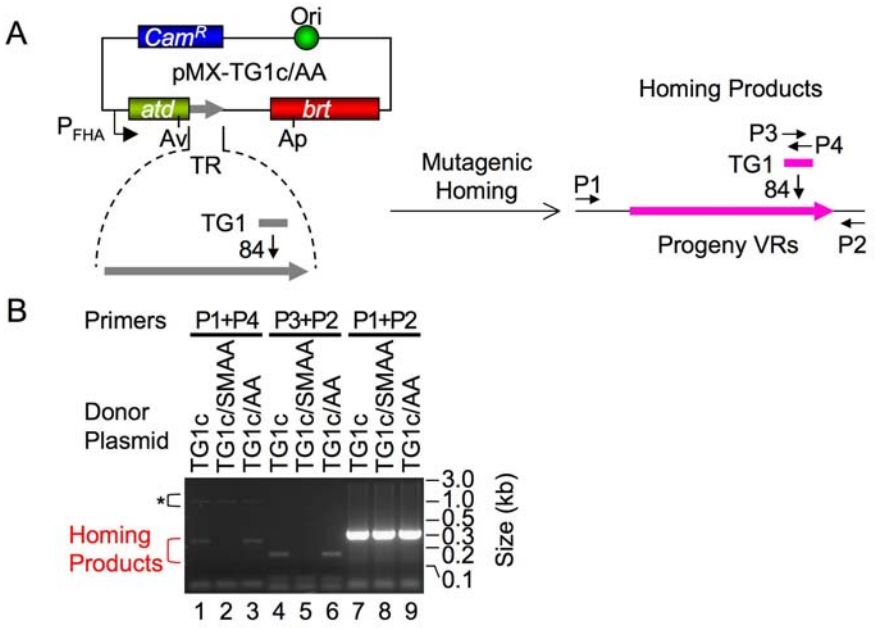

Figure S6. Silent mutations used to introduce AvrII and ApaI sites in *atd* and *brt* do not affect DGR function

(A) Donor plasmid pMX-TG1c/AA and its homing product. pMX-TG1c/AA is essentially the same as pMX-TG1c except for the AvrII (Av) and ApaI (Ap) sites introduced by silent mutations.

(B) Introduction of the AvrII and ApaI sites in *atd* and *brt* has no detectable effect on DGR homing. Homing assays were performed as in Figure 1C. TG1c, positive control pMX-TG1c; TG1c/SMAA, Brt-deficient derivative of pMX-TG1c; TG1c/AA, pMX-TG1c/AA. *, Brt-independent PCR artifact.

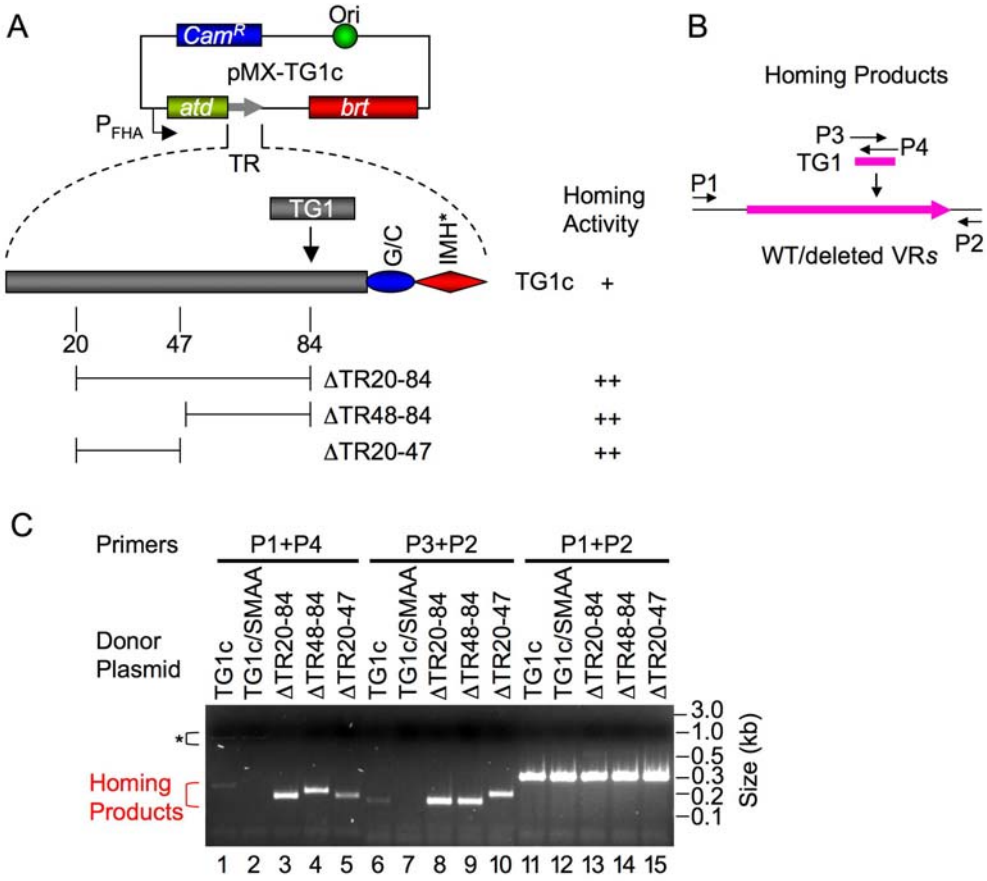

Figure S7. TR sequences between TG1a, TG1b and TG1c tag insertion sites are not required for DGR homing

(A) TR internal deletion constructs that delete regions between the tag insertion sites of TG1a and TG1c (ΔTR20-84), TG1b and TG1c (ΔTR48-84), and TG1a and TG1b (ΔTR20-47). The TG1 tag was inserted at the deletion junctions in all the constructs to facilitate homing assays. Homing activities analyzed in C are summarized to the right. +, homing activity of the positive control pMX-TG1c; ++, activities significantly above the positive control.

(B) Homing products and assay primers.

(C) Homing assays of TR internal deletion constructs in **(A)**. Assays were performed as in Figure 1C. TG1c, positive control pMX-TG1c; TG1c/SMAA, Brt-deficient negative control. *, Brt-independent PCR artifact.

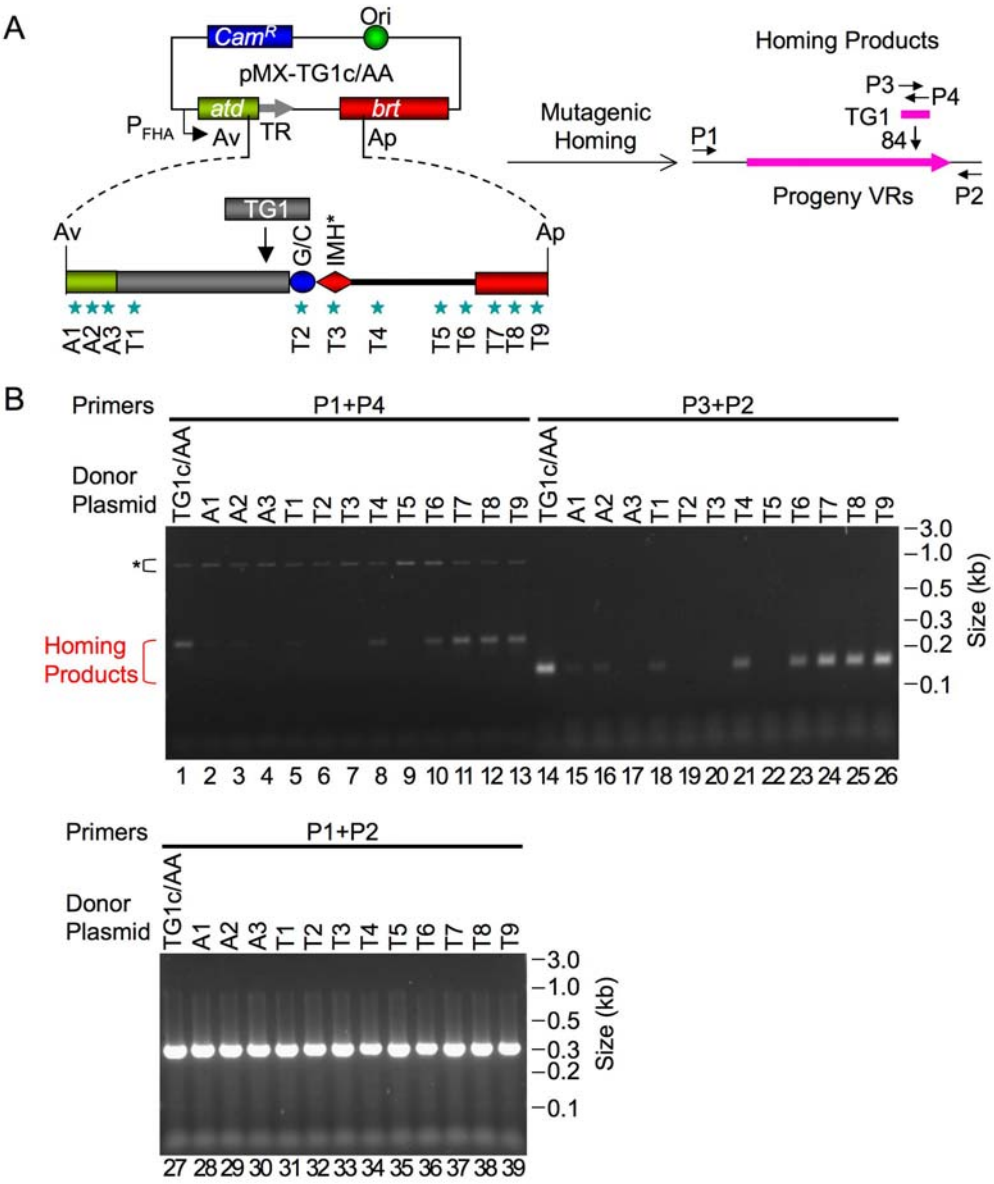

Figure S8. Silent mutation scanning to detect regions of the TR-containing RNA transcript important for DGR homing

(A) Locations of silent mutations in the donor constructs and their homing products. A1-3 are three different donors with silent mutations at the 3' end of *atd*, downstream of the AvrII (Av) site. T7-9 are three donors with silent mutations at the 5' end of *brt*, upstream of the ApaI (Ap) site. The *brt* ORF can potentially be extended at the 5' end to include the entire TR. T1-6 are donors with silent mutations in this extended ORF. The mutations in T1-3 are located in TR, while those in T4-6 are located in the spacer between TR and *brt*. Primers were described in Figure 1B.

(B) Effects of silent mutations A1-3 and T1-9 on DGR homing. Homing assays were performed as in Figure 1C. TG1c/AA, positive control pMX-TG1c/AA. *, Brt-independent PCR artifact.

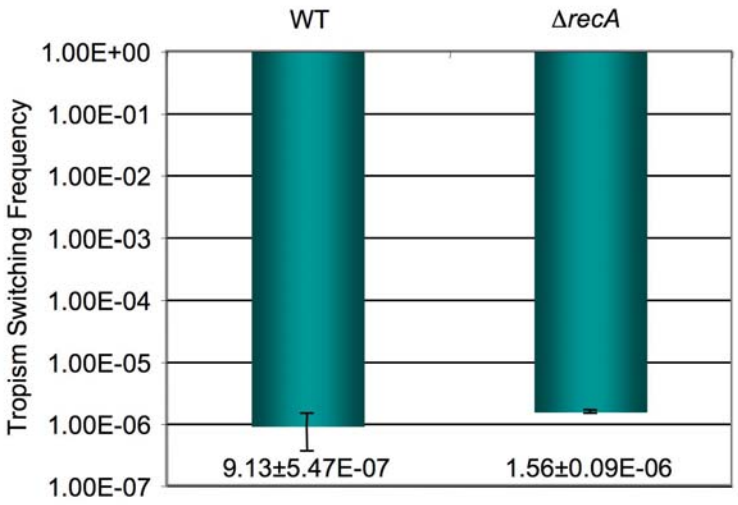

Figure S9. DGR-mediated phage tropism switching occurs independently of the host RecA-dependent homologous recombination function

Progeny phages were generated from phage BPP-1d through single-cycle lytic infection of wild type RB50 and RB50Δ*recA* cells harboring the homing-competent donor plasmid pMX1. Tropism switching frequencies were determined as the ratio of progeny phages that infect Bvg^- phase RB54 cells vs those that infect Bvg^+ phase RB53Cm cells. Data represent the mean of two independent experiments ± standard deviation. As negative controls, the Brt-deficient donor pMX1/SMAA failed to support BPP-1d phage tropism switching in either cell type with at least 2.8×10^9 progeny phages analyzed (data not shown).

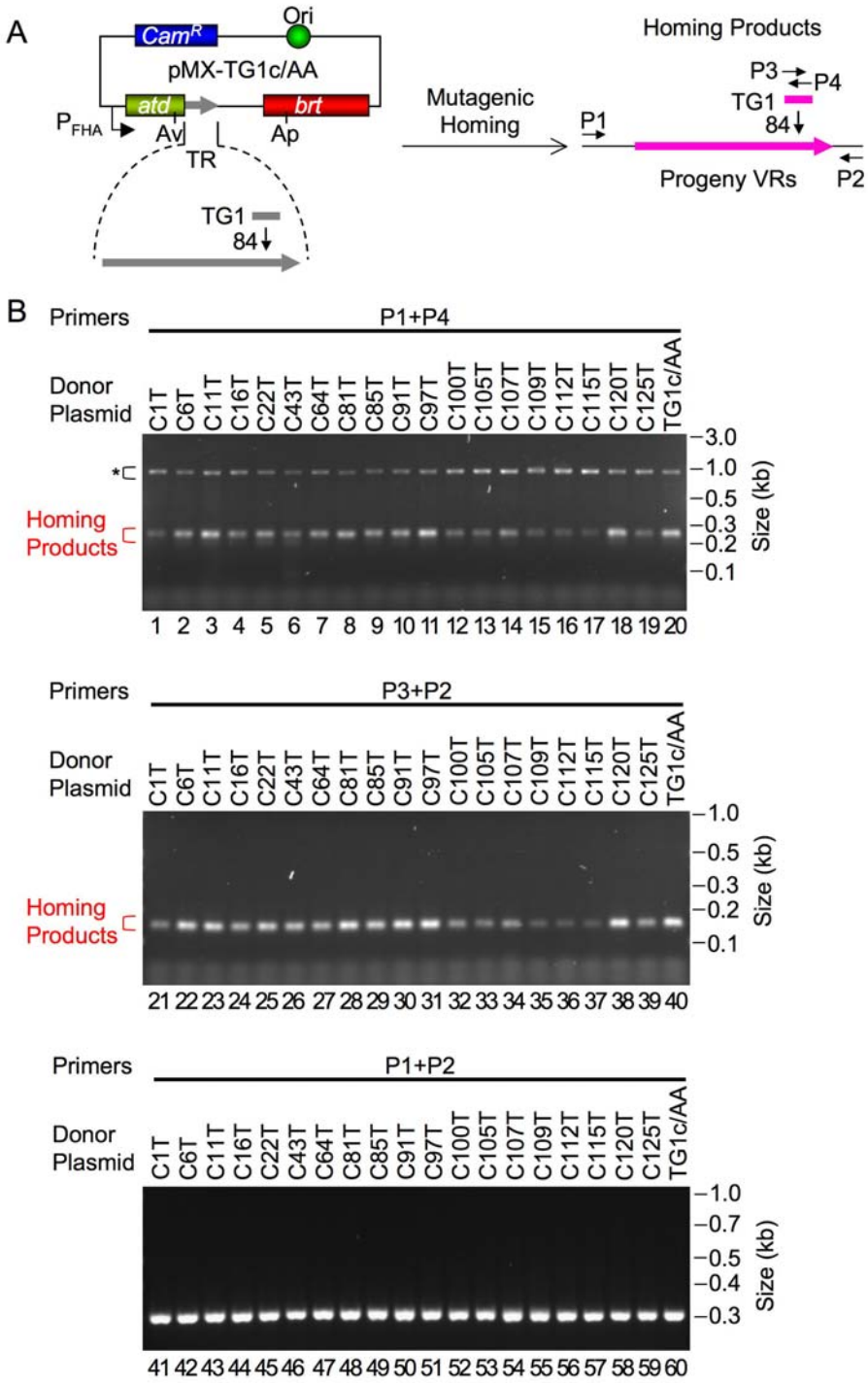

Figure S10. DGR homing assays to detect marker coconversion of donor VRs with different C to T markers in TR

(A) Donor plasmid pMX-TG1c/AA that was used for introduction of different C to T markers and its homing product.

(B) Donor plasmids containing different C to T markers in TR support DGR homing. TG1c/AA, positive control pMX-TG1c/AA. Other donors contain C to T markers at the indicated TR positions. *, Brt-independent PCR artifact.

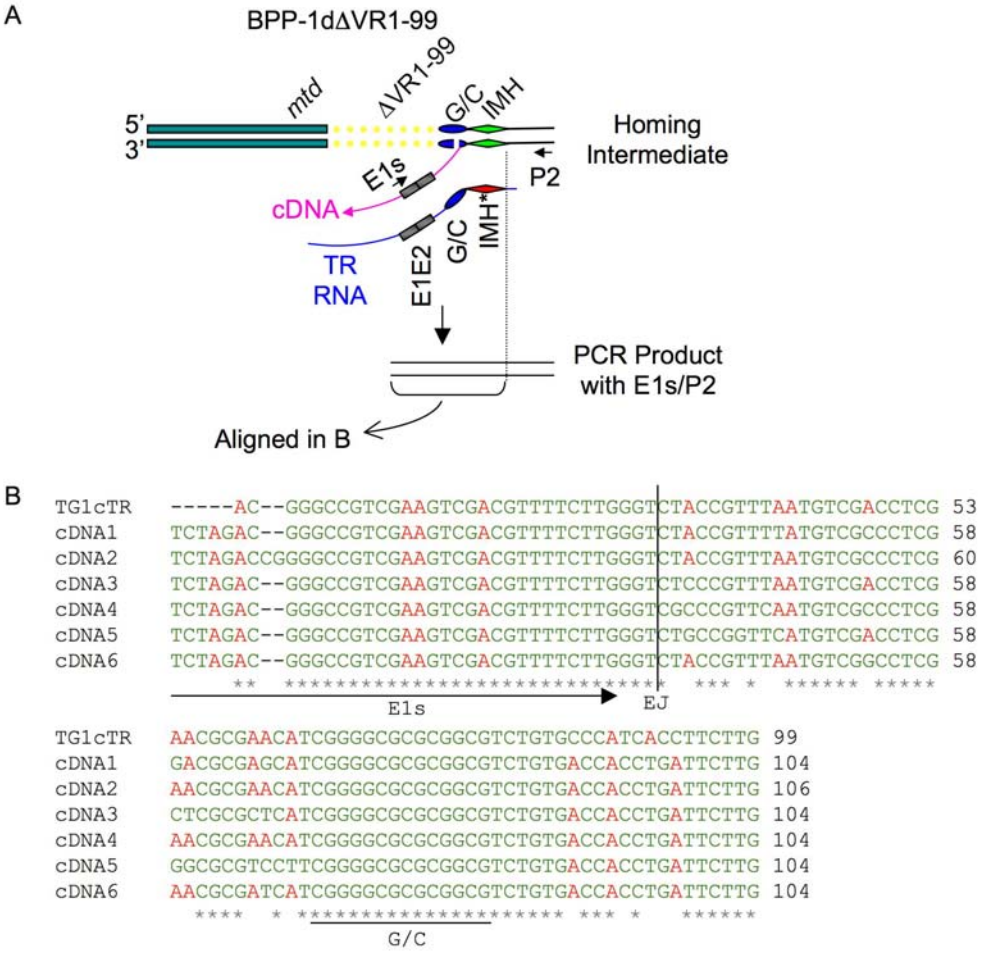

Figure S11. Sequence alignment of potential homing intermediates generated in BPP-1dΔVR1-99 lysogens expressing pMX-*td* show precise exon ligation and adenine mutagenesis

(A) A potential DGR homing intermediate and its detection by PCR. Homing intermediates were amplified with primers E1s and P2, and subsequently cloned and sequenced. Area of interest is aligned in **(B)**.

(B) Alignment of sequences of 6 independent cDNA clones with the corresponding TG1c TR sequence shows accurate exon joining and adenine mutagenesis. Primer E1s annealing site, exon junction (EJ) and the $(G/C)_{14}$ element are also indicated.

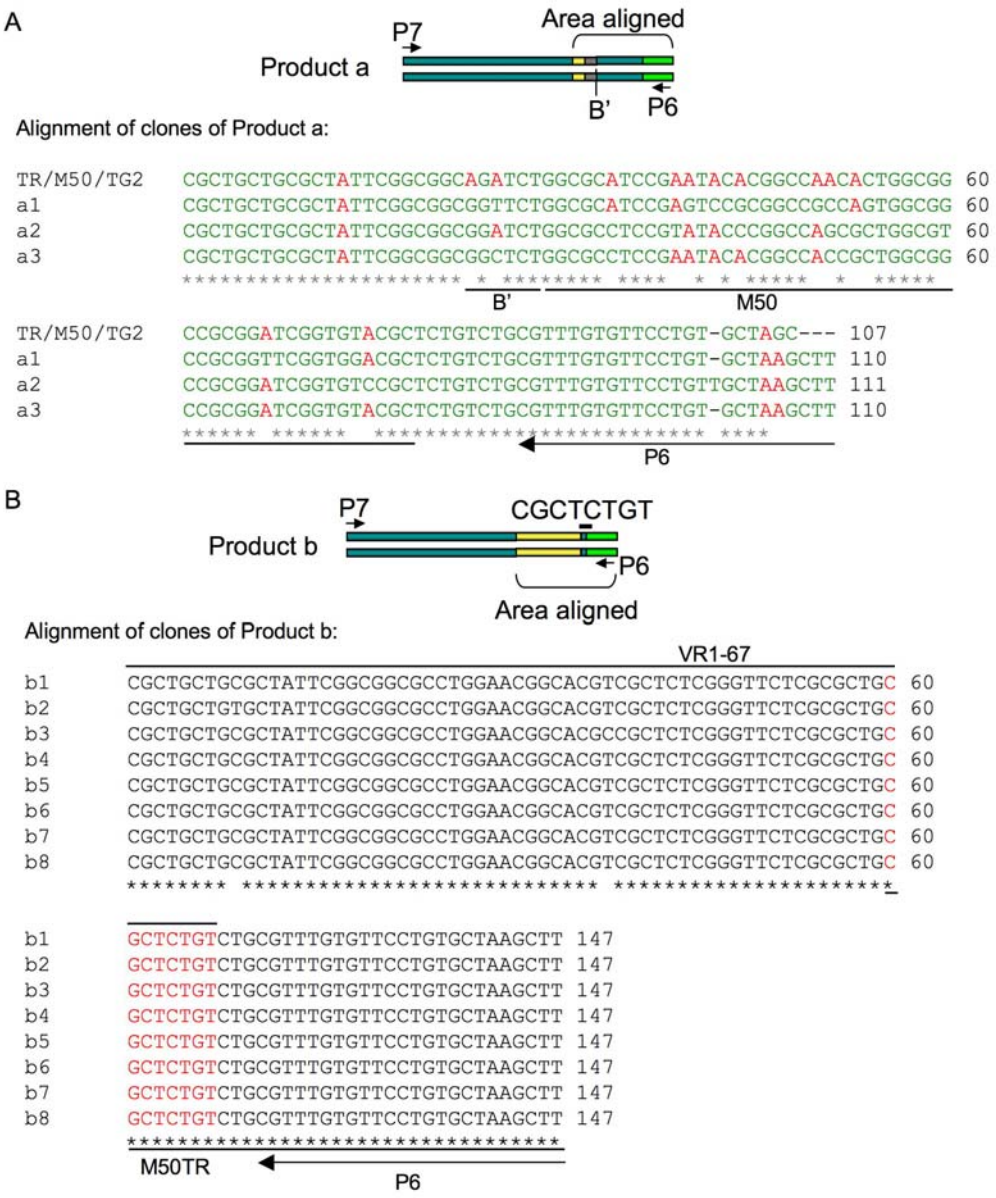

Figure S12. Sequences of products a and b from band 1 in lane 2 of Figure 6B
(A) Shown at top is a diagram of product a, generated with primers P7 and P6. Area of interest aligned below is also indicated. 3 independent clones of product a are aligned with the corresponding TR sequence of pMX-M50 to show adenine mutagenesis and to determine 5' cDNA integration sites. Primer P6 annealing site and M50 are also indicated. As the BglII site in TR was also transferred to VR and diversified, cDNA integration most likely occurred within the first 22 bp of the parental VR. B', diversified BglII site.
(B) Shown at top is a diagram of product b. The 8-nt sequence implicated in mediating 5' cDNA integration is shown. Area of interest aligned below is also indicated. 8 independent clones of product b are aligned. Judging from the boundary of phage- and plasmid-donated sequences, 5' cDNA integration appears to have occurred between VR positions 60 and 67 (shown in red), and was mediated by the homologous 8 nt sequence in TR of pMX-M50.

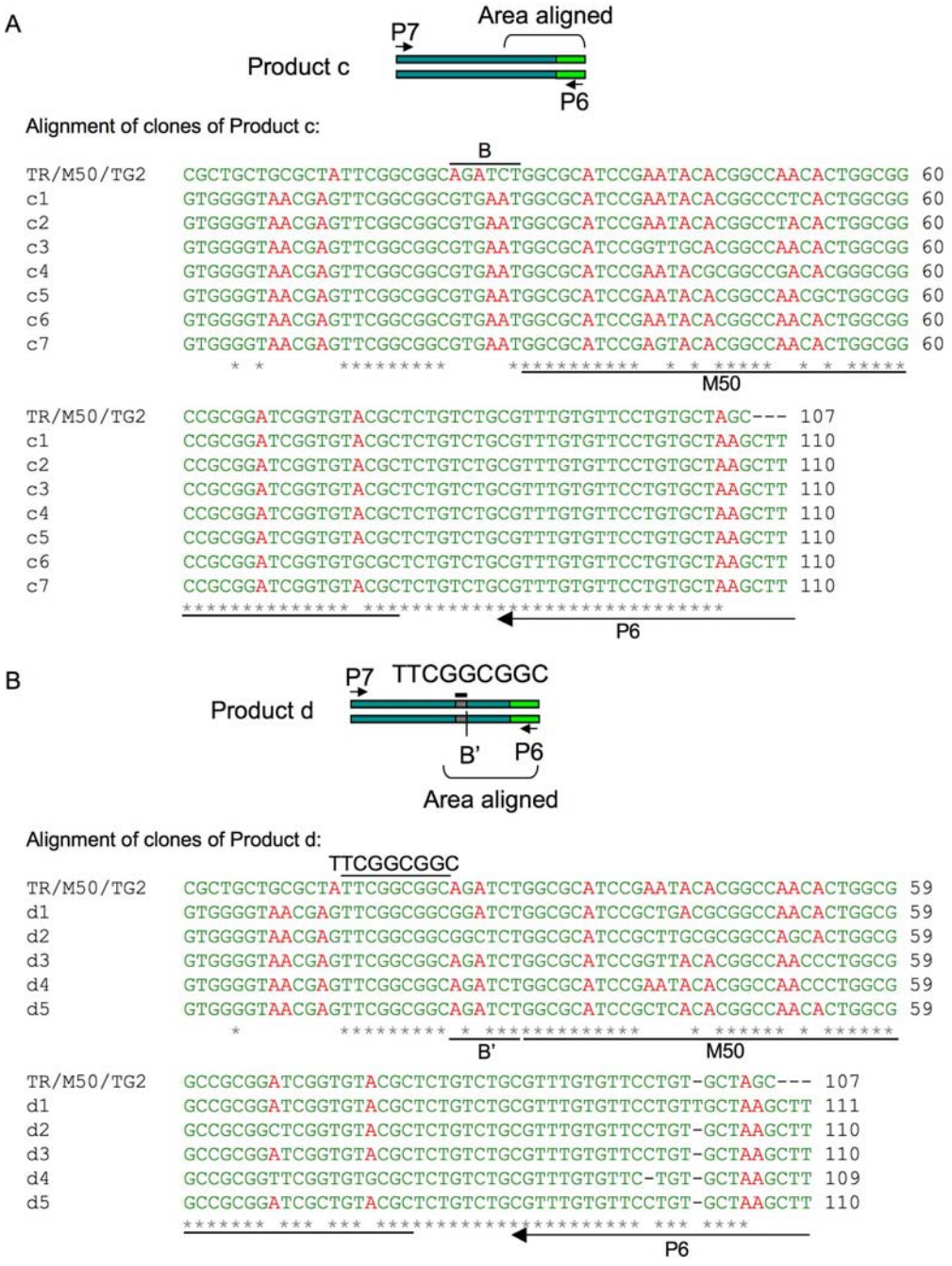

Figure S13. Sequences of products c and d of band 2 in lane 2 of Figure 6B
(A) Shown at top is a diagram of product c, generated with primers P7 and P6. Area of interest aligned below is indicated. 7 independent clones of product c are aligned with the corresponding TR sequence of pMX-M50 to show adenine mutagenesis and to determine 5' cDNA integration sites. As the BglII site in TR was not transferred to VR and adenine mutagenesis occurred within the M50 insert, cDNA integration most likely occurred within the M50 sequence of the phage *mtd* gene.

(B) Shown at top is a diagram of product d. The 9 nt sequence implicated in mediating 5' cDNA integration upstream of M50 in the *mtd* gene is shown. Area of interest aligned below is also indicated. 5 independent clones of product d are aligned with the corresponding TR sequence of pMX-M50 to show adenine mutagenesis and to determine 5' cDNA integration sites. As the BglII site was transferred from TR to VR and in two cases, diversified, and no TR sequences upstream of the 9 nt homology were transferred, 5' cDNA integration is concluded to have occurred within the 9 nt homologous sequence located 6 nt upstream of M50 in the phage *mtd* gene. B', diversified BglII site.

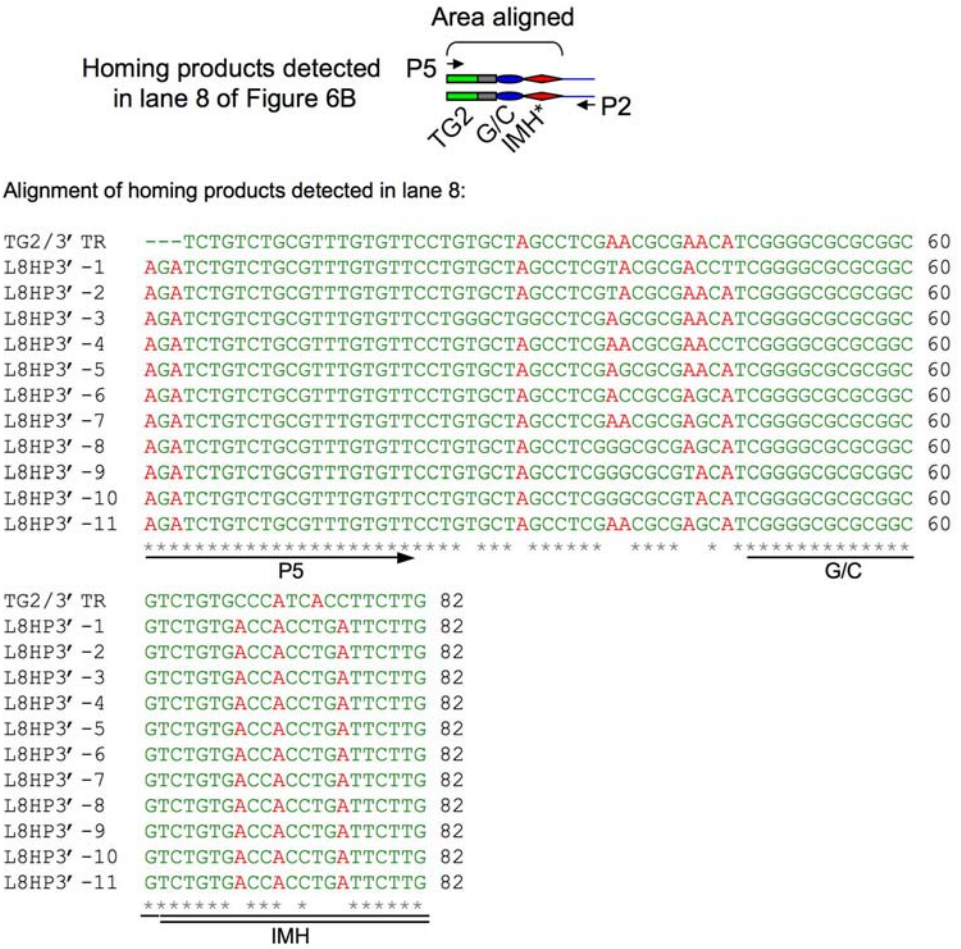

Figure S14. Alignment of pMX-M50 homing products in BPP-1d lysogens (detected in lane 8 of Figure 6B) with the corresponding TR sequence of the donor plasmid
Shown at top is a diagram of the homing product detected with PCR primers P5 and P2 in lane 8 of Figure 6B. Area of interest aligned below is indicated. Shown below is alignment of 11 independent homing products with the corresponding TR region of pMX-M50. $(G/C)_{14}$/IMH elements and primer P5 annealing site are indicated.

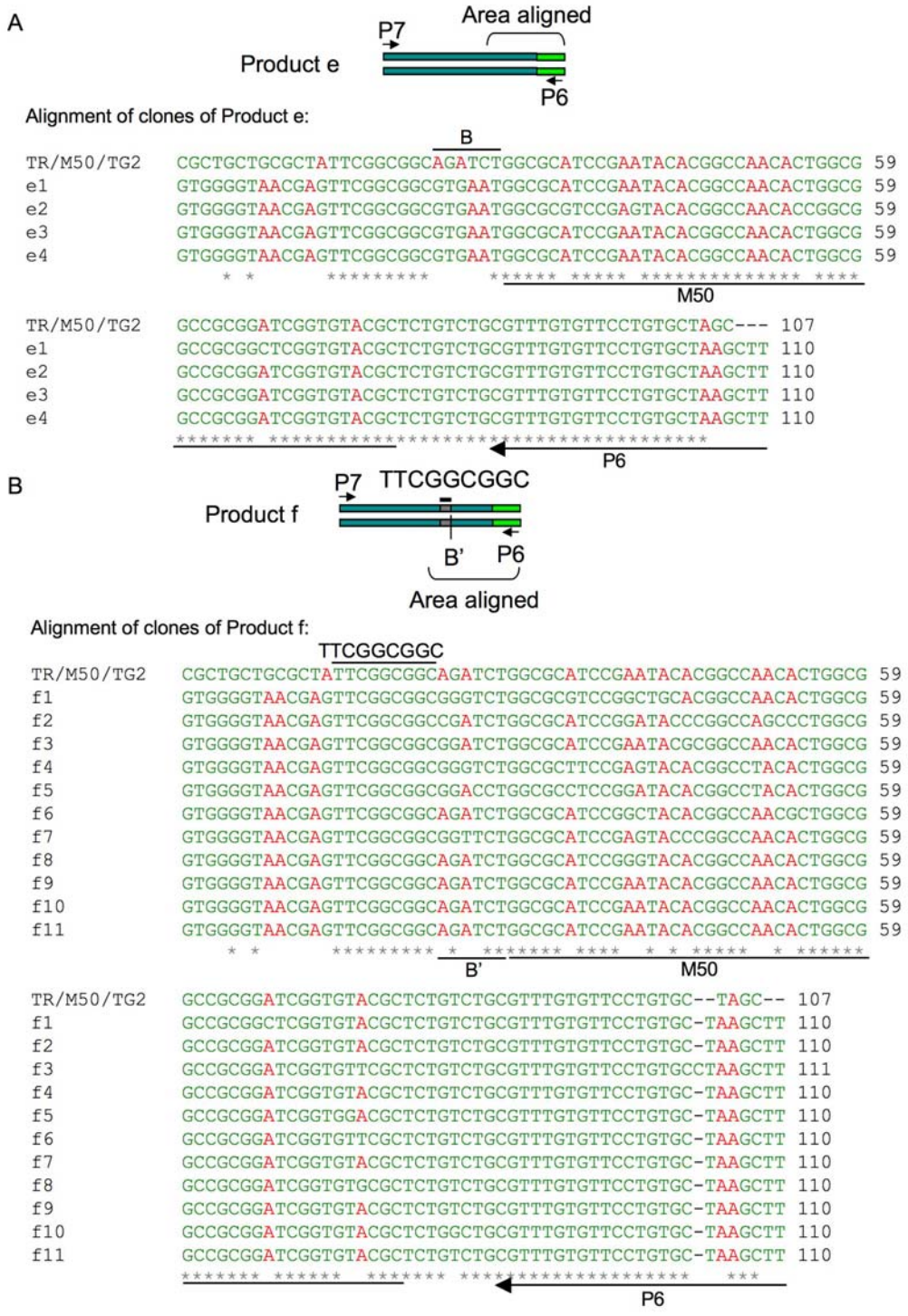

Figure S15. Sequences of products e and f of band 3 in lane 5 of Figure 6B
(A) Shown at top is a diagram of product e, which has a structure identical to product c. Area of interest aligned below is indicated. 4 independent clones of product e are aligned with the corresponding TR sequence of pMX-M50 to show adenine mutagenesis and to determine 5' cDNA integration sites. The BglII site in TR was not transferred to VR and adenine mutagenesis occurred within the M50 insert in two of the clones,

indicating that at least two of the clones are true homing products and that cDNA integration occurred within the M50 sequence of the phage *mtd* gene.
(B) Shown at top is a diagram of product f that is structurally identical to product d. 11 independent clones of product f are aligned with the corresponding TR sequence of pMX-M50. As the BglII site was transferred from TR to VR and in 6 cases, diversified, and no TR sequences upstream of the 9 nt homology were transferred, we conclude that 5' cDNA integration occurred within the 9 nt homologous sequence. B', diversified BglII site.

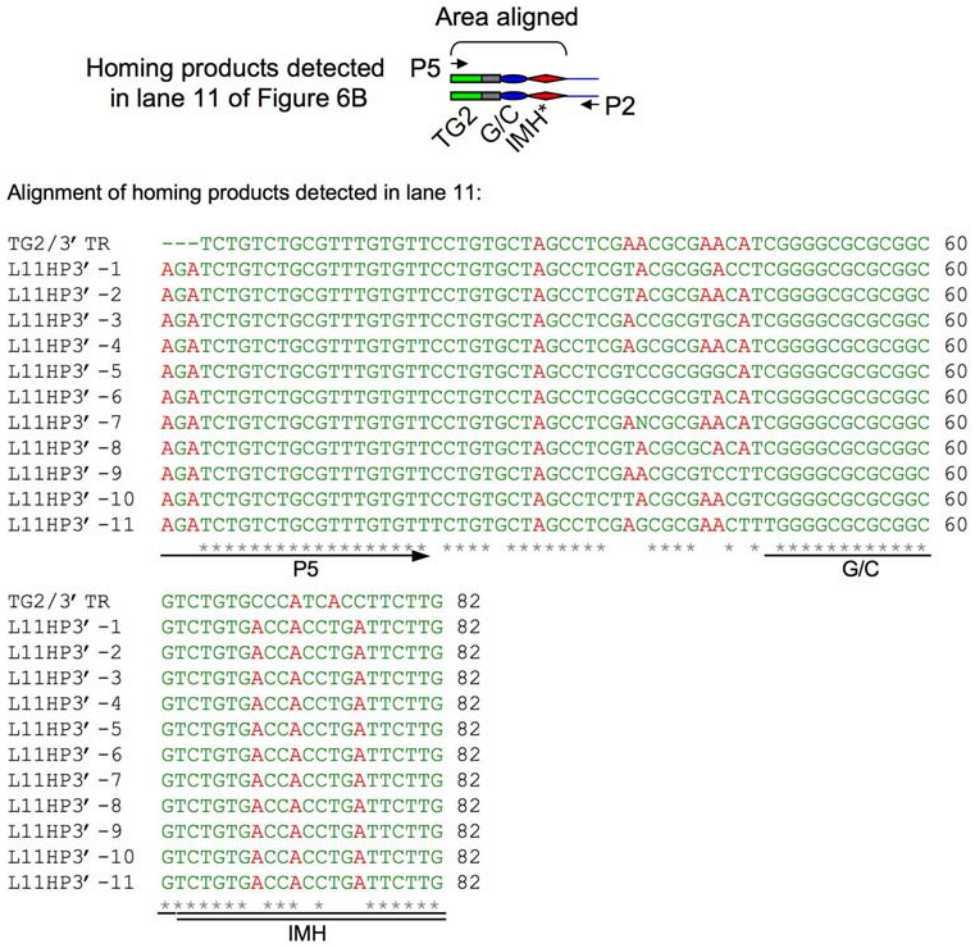

Figure S16. Alignment of pMX-M50 homing products in BPP-1dΔVR1-99 lysogen (detected in lane 11 of Figure 6B) with the corresponding TR sequence of the donor plasmid

Shown at top is a diagram of the homing products detected with PCR primers P5 and P2 in lane 11 of Figure 6B. Area of interest aligned below is indicated. Shown below is an alignment of 11 independent homing products with the corresponding TR sequence of pMX-M50. $(G/C)_{14}$/IMH elements and primer P5 annealing site are indicated.